Paper: ASAT-13-FM-04

13th International Conference on
AEROSPACE SCIENCES & AVIATION TECHNOLOGY,
ASAT- 13, May 26 – 28, 2009, E-Mail: asat@mtc.edu.eg
Military Technical College, Kobry Elkobbah, Cairo, Egypt
Tel : +(202) 24025292 – 24036138, Fax: +(202) 22621908

Trajectory Prediction for a Typical Fin Stabilized Artillery Rocket

M. Khalil*, H. Abdalla* and O. Kamal*

Abstract: This paper investigates the trajectory prediction and dispersion for unguided fin stabilized artillery rocket in order to explain the importance of the rocket production accuracy and the benefit of using guided rockets. The total dispersion results mainly from three effects. The first is the dispersion due to rocket production inaccuracy, which includes propellant mass, composition inaccuracy, rocket total mass, axial and lateral moments of inertia and resultant center of gravity. The second dispersion during boosting phase which includes launcher deflection, missile tip-off from the launcher, thrust and fin misalignments, and atmospheric disturbances such as tail wind, cross wind, and gusts. While the third is the dispersion during free-flight phase that is due to the fluctuations in wind profile.

In this study, a trajectory calculation using a 6-DOF model was developed and applied for a typical artillery rocket, the 122 mm artillery rocket, at different mass and flight properties to predict the trajectory parameters and dispersion.

Keywords: Dispersion Analysis, Nominal Trajectory, Trajectory Prediction, 6-DOF Model, 122mm unguided artillery rocket.

Nomenclature

$[a_N\ a_E\ a_D]^T$	Acceleration vector acting on the body.
C_A	Total axial force coefficient.
C_l	Total roll moment coefficient.
C_{lp}	Rolling moment coefficient derivative with roll rate.
C_{lr}	Rolling moment coefficient derivative with yaw rate.
C_{mq}	Pitching moment coefficient derivative with pitch rate.
$C_{m\alpha}$	Pitching moment derivative with rate of change of angle of attack.
$C_{m\dot{\alpha}}$	Pitching moment derivative with rate of change of angle of attack.
$C_{N\alpha}$	Normal force coefficient derivative with angle of attack
$C_{N\dot{\alpha}}$	Normal force coeff. derivative with rate of change of angle of attack
g	Normal gravity on the ellipsoidal surface.
I_x	Body axial moment of inertia, [kg.m^2].
I_{xy}, I_{yz}, I_{zx}	Body mass products of inertia, [kg/m^2].

* Egyptian Armed Forces

I_y, I_z	Body transverse moment of inertia, [kg.m^2].
L_{BE}	Transformation matrix from earth frame F_E to body frame F_B.
M	Mach number.
m	Total mass of the body, [kg].
p	Body spin rate, [rad/s].
$[P\ Q\ R]^T$	Body angular velocity, [rad/s].
q	Body pitch rate, [rad/s].
r	Body yaw rate, [rad/s].
$[T_x\ T_y\ T_z]^T$	Components of the resultant external force acting on the body in the body fixed reference frame, [N].
$[u\ v\ w]^T$	Components of the velocity vector of the body in the body fixed reference frame, [m/s].
$[\dot{V}_N\ \dot{V}_E\ \dot{V}_D]^T$	Total acceleration vector acting on the body.
α	Angle of attack.
β	Angle of sideslip.
γ	Specific heat ratio ($\gamma = 1.4$ for isentropic flow).
φ	Roll angle (Bank angle) [deg].
λ	The latitude of body C.G w.r.t. Earth fixed reference frame [rad].
μ	Longitude of body C.G w.r.t. earth fixed reference frame [rad].
θ	Pitch angle (inclination angle), [deg].
ψ	Yaw angle (azimuth angle), [deg].
ω^E	Angular velocity of the earth $[p^E\ q^E\ r^E]^T$ about the inertia reference frame [rad/s].

1. Introduction

Simulation of the trajectory of unguided rockets is a combination between all characteristics of the rocket (e.g. mass properties and configuration) and atmospheric conditions (predicted values). In practice, there are some differences between the real and the nominal trajectory due to manufacturing, measurement and atmospheric modeling errors. These differences make the rocket deviates from its nominal trajectory and miss its target.
Therefore, studying sources of error between the real and predicted trajectories is a must, in order to help rocket designers to optimize the manufacturing tolerances and restrictions to avoid these sources of error, [8].

The total dispersion results mainly from three phases [1, 2, 3]:

- Dispersion due to rocket production inaccuracy, which includes:
  - The propellant mass and composition inaccuracy.
  - The rocket total mass, axial and lateral moments of inertia and resultant center of gravity inaccuracies.
- Dispersion during boosting phase:
  - Launcher deflection: It is the most common factor present with long launchers. It results from ignition shock and sudden high thrust build-up from the booster, which will generate a pitching rate on the rocket and it can be

solved by: (1) designing a stiffer launcher, (2) accounting for this motion in setting the launcher.

- Rocket tip-off from the launcher: if the supporting shoes on the missile do not leave the supporting rail or rails simultaneously, this will tilt the rocket downward under the force of gravity and cause the missile to fly a new flight path. With simultaneous shoe release, the rocket would have a simple translational instead of combined translational and rotational motion immediately upon leaving the launcher. This translational motion is not as detrimental to the dispersion as the rotational motion.
- Launcher setting: since it is physically impossible to set the launcher precisely at the desired angle, error in launcher angle is always present.
- Variation in rocket motor performance: because of the tolerance in rocket-motor design, propellant properties, and manufacturing, the total impulse of the rocket motor may vary.
- Thrust and fin misalignments: it is an important source of dispersion in case of unguided rockets "flying on open loop". To minimize the dispersion due to this misalignment a large static stability margin is required but its not desired if the rocket is launched in a cross wind. Another method is used widely which is spinning the rocket immediately off the launcher. This initial spin may be produced by spin motor mounted on the missile or by using helical-rail launchers.
- And atmospheric disturbances such as tail wind, cross wind, and gusts.

- Dispersion during free-flight phase, which caused from change in wind profile, variation in atmospheric density and variation in rocket characteristics.

2. Mathematical Model

In order to predict the trajectory of an unguided artillery rocket, six degrees of freedom 6-DOF mathematical model is presented in [1,6], where the block diagram of this model is shown in Fig. 1.

The equations of motions that describe the 6-DOF model are derived according to some assumptions:

a) The flying body is rigid.
b) All equations are referred to a body fixed reference frame.
c) The aerodynamic coefficients are calculated in body fixed reference frame.
d) The Earth model is included (ellipsoidal shape, rotation, gravity....).
e) The atmospheric model is included where the temperature, sonic speed, and air density are varying with the body altitude.

The 6-DOF equations of motions are three translational degrees describe the motion of mass (CG), also called the trajectory, as shown in equation (1),

$$\begin{bmatrix} \dot{u} \\ \dot{v} \\ \dot{w} \end{bmatrix} = \left(\frac{1}{m}\right)\begin{bmatrix} T_x - A_{axial} \\ T_y + A_{side} \\ T_z - A_{normal} \end{bmatrix} + g\begin{bmatrix} -\sin\theta \\ \cos\theta.\sin\varphi \\ \cos\theta.\cos\varphi \end{bmatrix} + \begin{bmatrix} p_B^E + p \\ q_B^E + q \\ r_B^E + r \end{bmatrix} \times \begin{bmatrix} u \\ v \\ w \end{bmatrix} \quad (1)$$

And three attitude degrees orient the projectile, as shown in equation (2),

$$\dot{p} = \left(\frac{L}{I_x}\right) + \left(\frac{I_{zx}\left(\dot{r} + p.q\right)}{I_x}\right) + \left(\frac{\left(I_y - I_z\right).q.r}{I_x}\right)$$
$$\dot{q} = \left(\frac{M}{I_y}\right) + \left(\frac{I_{zx}\left(r^2 - p^2\right) + \left(I_z - I_x\right).r.p}{I_y}\right) \qquad (2)$$
$$\dot{r} = \left(\frac{N}{I_z}\right) + \left(\frac{I_{zx}\left(\dot{p} - q.r\right)}{I_z}\right) + \left(\frac{\left(I_x - I_y\right).p.q}{I_z}\right)$$

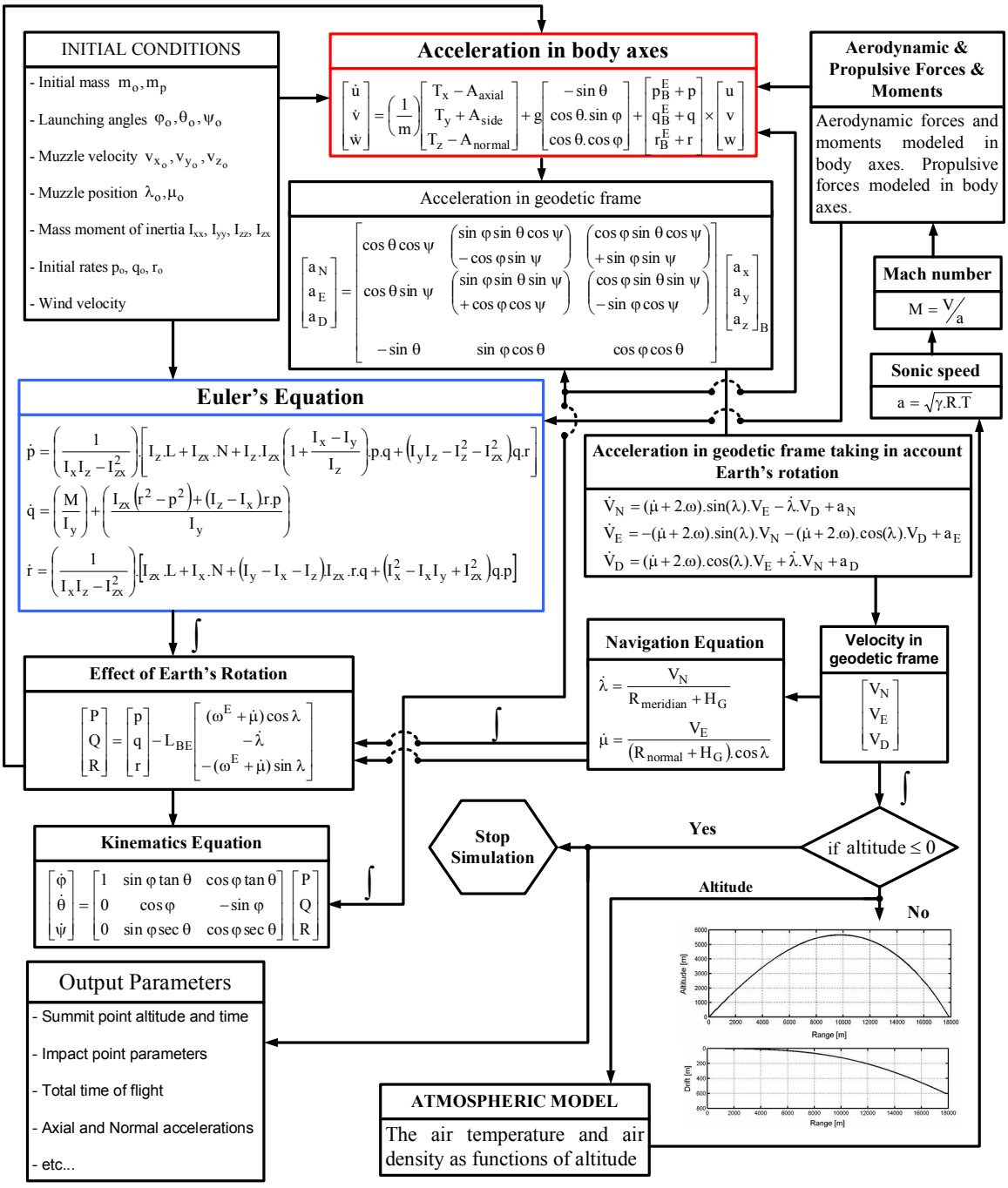

Fig. 1 Block diagram of 6-DOF model

The Earth rotation is taken into consideration as,

$$\begin{bmatrix} P \\ Q \\ R \end{bmatrix} = \begin{bmatrix} p \\ q \\ r \end{bmatrix} - L_{BE} \begin{bmatrix} (\omega^E + \dot{\mu})\cos\phi \\ -\dot{\lambda} \\ -(\omega^E + \dot{\mu})\sin\phi \end{bmatrix} \tag{3}$$

where the transformation matrix from body axes to earth axes is shown in equation (4),

$$L_{BE} = \begin{bmatrix} \cos\theta\cos\psi & \cos\theta\sin\psi & -\sin\theta \\ \begin{pmatrix}\sin\varphi\sin\theta\cos\psi \\ -\cos\varphi\sin\psi\end{pmatrix} & \begin{pmatrix}\sin\varphi\sin\theta\sin\psi \\ +\cos\varphi\cos\psi\end{pmatrix} & \sin\varphi\cos\theta \\ \begin{pmatrix}\cos\varphi\sin\theta\cos\psi \\ +\sin\varphi\sin\psi\end{pmatrix} & \begin{pmatrix}\cos\varphi\sin\theta\sin\psi \\ -\sin\varphi\cos\psi\end{pmatrix} & \cos\varphi\cos\theta \end{bmatrix} \tag{4}$$

3. Case Study

In this study, a trajectory calculation using a 6-DOF model was developed and applied for 122 mm unguided artillery rocket. All aerodynamic forces and moments coefficients of the given shell are calculated using *Missile Datcom*. The mass properties of the given shell is calculated using *Inventor* considering the change of the rocket mass during propellant burning till the propellant burn-out (active part), then the rocket will fly the rest of its trajectory as a projectile of fixed mass (passive part). The 6-DOF model assumed the rocket is ideal, where the axis of symmetry of the exterior surface coincides with the longitudinal principal axis of inertia, and the two lateral principal moments of inertia are identical.

3.1. Main data

The main data and firing conditions of the studied artillery rocket are summarized below:

Caliber.	D	=	122 mm
Overall Length.	L_t	=	2870 mm
Total Mass.	M_t	=	66 Kg
Propellant Mass.	m_p		20.5 Kg
Propellant Burning Time.	t_k		1.67 s
Mean Thrust.	T_x		23600 N
Initial Center of Gravity from the Nose Tip.	$C.G\_x_i$	=	1.374 m
Final Center of Gravity from the Nose Tip.	$C.G\_x_f$	=	1.264 m
Initial Axial Moment of Inertia.	I_xx_i	=	0.1499 Kg.m^2
Final Axial Moment of Inertia.	I_xx_f	=	0.1238 Kg.m^2
Initial Lateral Moment of Inertia.	$I\_yy_i = I\_zz_i$	=	41.58 Kg.m^2
Final Lateral Moment of Inertia.	$I\_yy_f = I\_zz_f$	=	33.83 Kg.m^2
Shell muzzle velocity	V_o	=	26.7 m/s
Shell muzzle spin rate	p_o	=	5.8 rps
Firing Elevation Angle	θ_o	=	50°

3.2. Aerodynamic coefficients and derivatives

Knowing the aforementioned configuration definitions, the aerodynamic coefficients and derivatives for 122mm unguided rocket are computed using the analytical capability of the Missile Datcom code. The results of these calculations are shown in Table 1.

Table 1 The aerodynamic coefficients and derivatives for 122mm unguided rocket

M	C_A		C_{N_α}	$C_{N_{\dot\alpha}}$	C_l	C_{l_p}	C_{l_r}		C_{m_α}		C_{m_q}		$C_{m_{\dot\alpha}}$	
	A	P					A	P	A	P	A	P	A	P
0.2	.340	.477	8.57	-52.129	.075	-8.198	0.161	-0.43	-53.8386	-61.6158	-2542.92	-2862.61	-96.593	-121.264
0.4	.305	.442	9.10	-52.139	.076	-8.312	0.219	-0.415	-54.3829	-62.2050	-2546.69	-2860.55	-99.443	-126.039
0.6	.291	.427	9.48	-52.148	.077	-8.449	0.225	-0.457	-55.1018	-62.9840	-2539.2	-2843.26	-104.587	-134.617
0.8	.290	.424	9.82	-52.157	.076	-8.448	0.437	-0.123	-54.3483	-62.1768	-2473.68	-2777.00	-112.628	-147.939
1.0	.391	.574	9.99	-52.63	.077	-8.339	0.615	0.294	-55.0595	-63.0754	-2423.07	-2735.95	-123.998	-166.608
1.1	.445	.648	10.16	-52.994	.094	-8.674	0.67	0.171	-62.072	-70.4885	-2675.52	-3000.02	-131.225	-178.402
1.2	.444	.637	10.00	-53.057	.102	-8.870	0.79	0.356	-65.6489	-74.3189	-2780.73	-3117.29	-140.089	-192.844
1.3	.349	.537	10.08	-63.529	.110	-9.304	0.871	0.551	-66.055	-75.5352	-2877.06	-3237.14	-144.48	-201.76
1.4	.345	.529	10.34	-65.882	.123	-10.17	0.974	0.793	-73.4021	-83.6276	-3068.43	-3463.90	-147.441	-206.842
1.5	.333	.512	10.44	-66.966	.128	-9.947	-0.807	-0.903	-70.0033	-80.0419	-2280.63	-2535.50	-148.807	-209.186
1.6	.322	.495	10.59	-67.717	.126	-9.836	-0.565	-1.079	-68.1121	-78.0571	-2282.44	-2535.58	-149.751	-210.807
1.8	.304	.464	10.67	-68.599	.120	-9.339	-0.688	-1.022	-63.0248	-72.6351	-2175.18	-2410.93	-150.862	-212.714
2.0	.287	.434	10.13	-68.875	.113	-8.762	-0.374	-0.536	-57.607	-66.8122	-2188.04	-2431.46	-151.209	-213.309
2.2	.271	.406	9.05	-68.672	.105	-8.15	0.064	-0.076	-37.6782	-45.2677	-1840.82	-2046.55	-150.953	-212.870

3.3. Trajectory Analysis

In order to investigate the trajectory parameters which are calculated using presented 6-DOF model of the given unguided rocket, a single case will be chosen corresponds to firing angle $\theta_o = 50°$.

Figure 2 shows the trajectory of the rocket at $\theta_o = 50°$. The rocket has very small drift in case of no side wind due to its high stability (fin stabilized). Figure 3 shows the rocket altitude during flight time, where the total flight time is 79 sec but the summit time is nearly 36 sec. Due to the high velocity of the rocket at the burn out point of the trajectory (at the end of burning), the summit time is less than half of the total flight time.

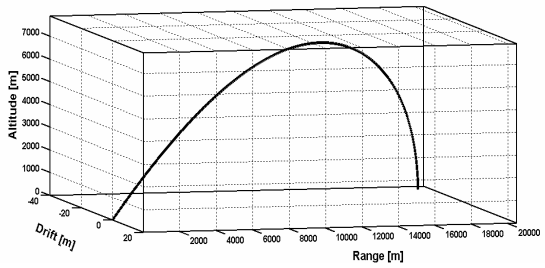

Fig. 2 The 3D trajectory path

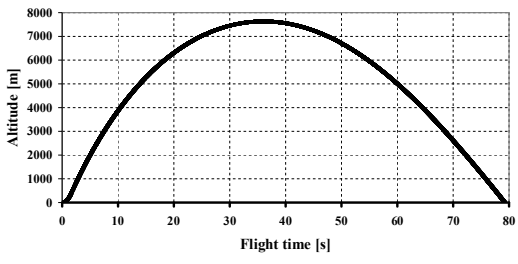

Fig. 3 The rocket altitude during flight time

Figure 4 shows the velocity of the rocket from firing to impact points, where the velocity at the firing point is 26.7 m/s and it will be increased due to the thrust force acting in flight direction, where the velocity at the burn-out point (end of burning) is 705 m/s. Then the

velocity will be decreased as well as the rocket goes up (altitude increased) until the summit point, then the rocket will go down to increase the rocket velocity due to a gravitational acceleration component in the direction of the velocity vector which will accelerate it.

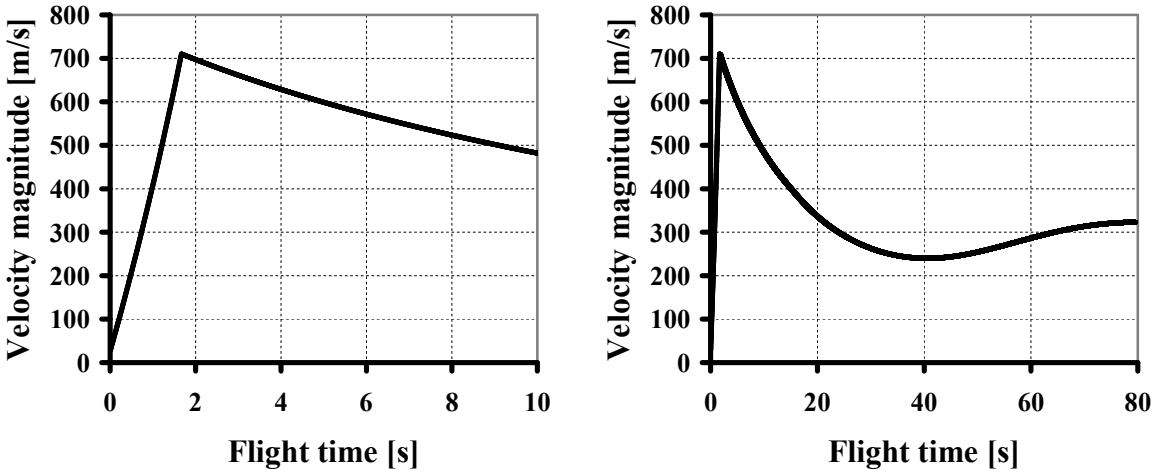

(a) **(b)**

Fig. 4 The velocity magnitude of the rocket vs. flight time

Figure 5-a shows the axial acceleration of the rocket at the beginning (firing point) where it is equal 35.4g in flight direction, due to the thrust force act in the axial direction of the rocket. The axial acceleration is increasing till the burn out point (end of burning) where the thrust equal zero then the axial acceleration is now 4g in direction opposite to its flight direction, due to the aerodynamic axial force acting on the rocket and the gravitational acceleration component in the opposite direction of its flight direction. Figure 5-b shows that the axial acceleration will be decreased due to the decreasing of its aerodynamic axial force (due to decreasing of free stream velocity) and decreasing of gravitational acceleration component in the opposite direction of flight direction (elevation angle is decreasing). The axial acceleration will be in the direction of flight again after the summit point, where the component of gravitational force is greater than the aerodynamic axial force and then it will be decreased again due to increasing of its aerodynamic axial force (increasing of free stream velocity).

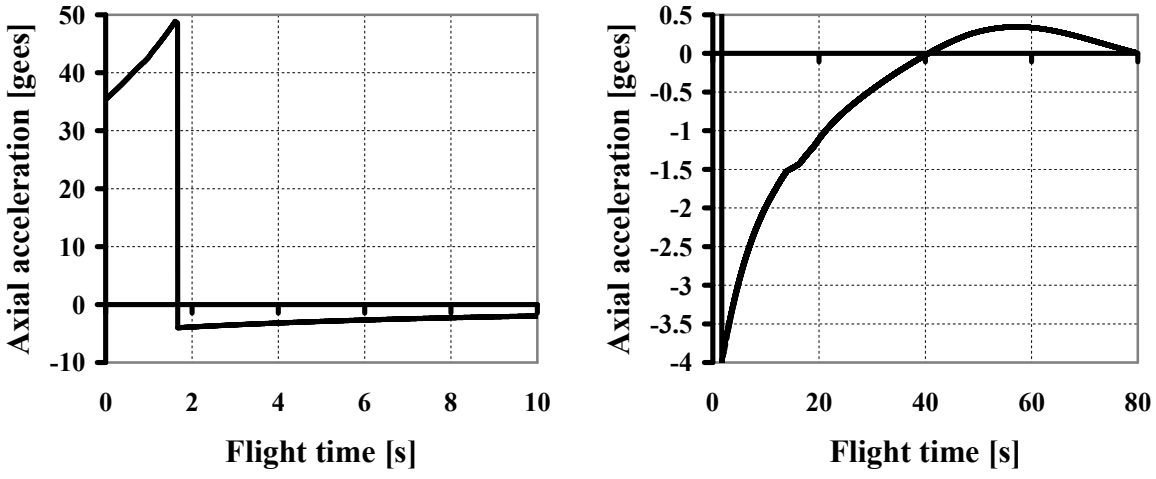

(a) **(b)**

Fig. 5 The axial acceleration of the rocket vs. flight time

Figure 6-a shows the normal acceleration from the point of firing till 10 s flight time, where the magnitude at the firing point is 0.64g. The normal acceleration is oscillating highly during the first 4 seconds, which may be attributed to oscillations of the aerodynamic rates.

Figure 6-b shows that the normal acceleration is increasing due to the decrease in the elevation angle of the rocket (increasing the gravitational acceleration component normal to rocket body) till the summit point of the rocket where the elevation angle is equal to zero to equal 1g and then the normal acceleration will decrease due to the increase of the elevating angle (decreasing the gravitational acceleration component normal to rocket body).

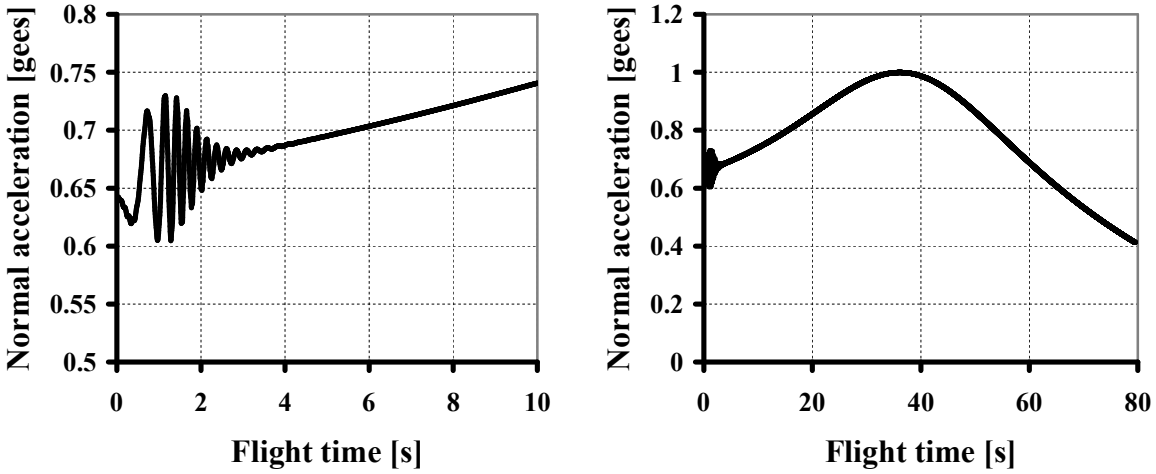

(a) **(b)**

Fig. 6 The normal acceleration of the rocket vs. flight time

Figure 7 shows the spin rate of the given rocket as function of flight time, where the spin rate at the firing point is 36 rad/s [5-6 rps] and then it will be decreased slightly after leaving launcher due to friction acting on the rocket body and the low velocity of the rocket. As the velocity of the rocket increased during burning of propellant, the spin rate will be increased due to the inclination of the rocket fins which will rotate the rocket in a positive spin direction as it shown in Fig. 7-a. After the burn-out point the rocket velocity will be decreased which will decrease the spin rate as shown in Fig. 7-b. Finally, the velocity will increase again to increase the spin rate too.

Figure 8 shows the variation of the elevation angle of the rocket during flight time, where the summit point is occurred nearly 36s. During the beginning of rocket flight there are fluctuations in the pitch angle as shown in Fig. 8-a due to the high pitch rate as shown in Fig. 9.

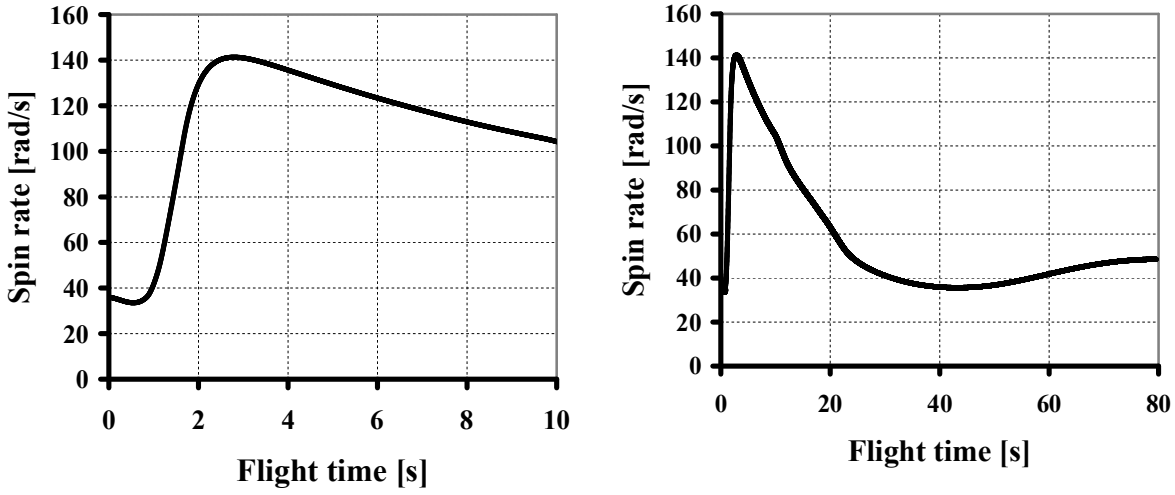

Fig. 7 The spin rate of the rocket vs. flight time

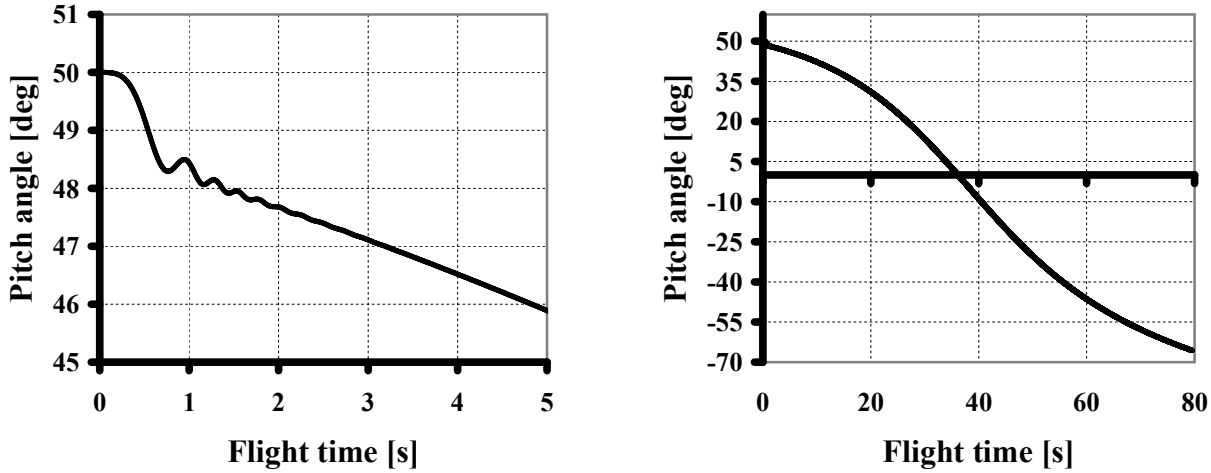

Fig. 8. The pitch angle of the rocket vs. flight time

Figure 9 shows the aerodynamic angles which are angle of attack α, side-slip angle β, and total angle of attack acting on the rocket during its flight time. Figure 9-a shows that the total angle of attack is zero at the launch point (no perturbation) and then increased and decreased in a cyclic motion with a high total angle of attack due to the rocket low velocity. As the velocity of the rocket increased to its maximum value at the burn out point at ($t = 1.67$ s), the total angle of attack fluctuation will be terminated. The total angle of attack will be increased as shown in Fig. 9-c till the summit point of the rocket, then it will be decreased till the end of flight.

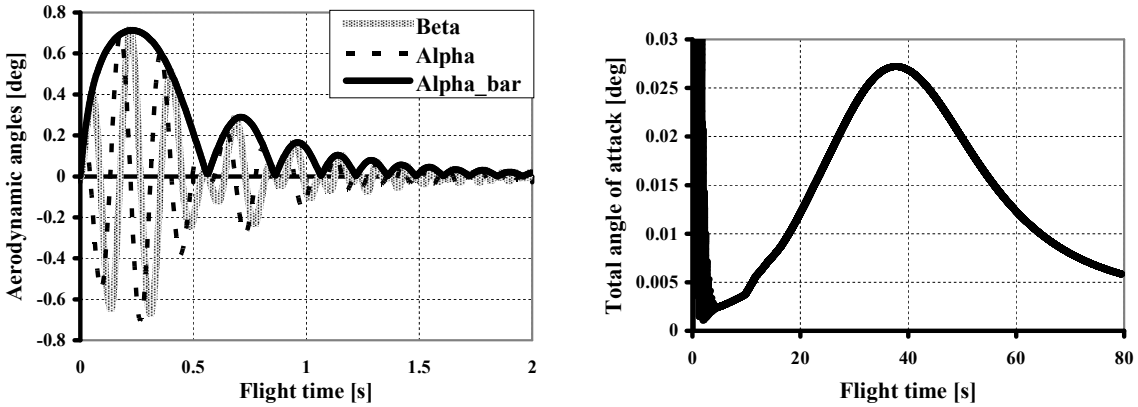

(a) **(b)**

Fig. 9. The aerodynamic angles of the rocket vs. flight time

3.4. Dispersion Analysis

The dispersions investigated in this paper have been applied to the rocket dynamics. The models modified in the rocket simulation to include dispersion capabilities which are firing conditions, and rocket mass properties. Table 2., shows a list of eight uncertainty parameters that have been used in this work. It is tried to consider all the important parameters.

The limits of uncertainties presented in table 2 are improved by individual error analysis, where a range of values in the defined limits in table 2, was given to each parameter and simulation was run several times. Using simulation results, it was possible to plot the impact point distance error vs. different parameters variation. This investigation is done in order to find a good estimation for each individual parameter uncertainty.

Table 2 Uncertainty parameters and ranges

	Parameter Definition	Uncertainty Range	Unit
1	Launching pitch angle	[-0.4 0.4]	deg
2	Rocket total mass	[-1.0 1.0]	%
3	Propellant mass	[-1.0 1.0]	%
4	Propellant burning time	[-0.1 0.1]	s
5	Thrust mean value	[-1.0 1.0]	%
6	Air density	[-4.0 4.0]	%
7	Axial moment of inertia	[-2.0 2.0]	%
8	Lateral moment of inertia	[-2.0 2.0]	%
9	Rocket launch velocity	[-2.0 2.0]	%
10	Rocket launch spin rate	[-2.0 2.0]	%
11	Wind speed at zero altitude	[-2.0 2.0]	m/s
12	Wind direction at zero altitude	[-2.0 2.0]	deg

The rocket dispersion is obtained from calculating range and drift differences from the projectile nominal point of impact. The effects of rocket launch velocity error on dispersion as shown in Fig. 10, is caused by the change of gases pressure applied on the base of the projectile due to the propellant ignition. The rocket range is inverse proportional to atmospheric density where the drag force is increased with the increasing of atmospheric density.

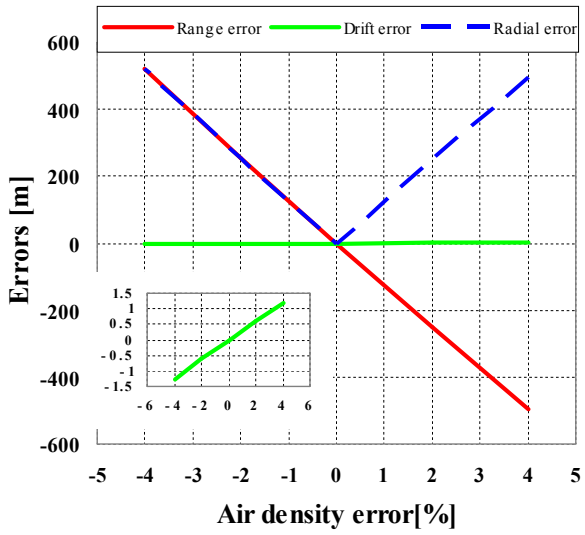

Fig. 10. The effect of air density error on dispersion

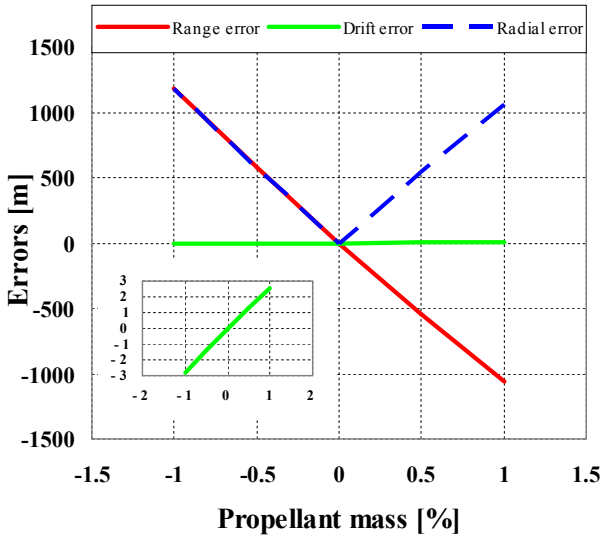

Fig. 11. The effect of propellant mass error on dispersion

The range is decreased with the increasing of the propellant mass as shown in Fig. 11 where the inertial force is less than in case of nominal trajectory during free flight regime, but the drift is slightly increased due to the increase of the gyroscopic moment. As the burning time of the rocket motor increased the range error increased due to the increase of the burn-out velocity as shown in Fig. 12, but the drift error is slightly decreased. Increasing the mean thrust value acting on the rocket will increase the rocket range error which also increases the burn-out velocity as shown in Fig. 13.

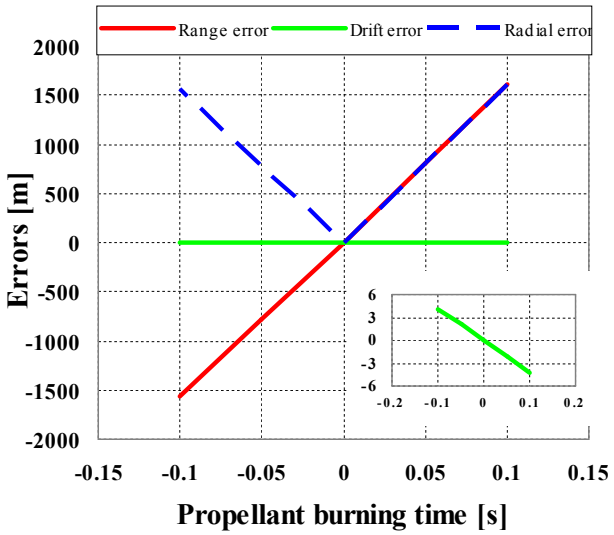

Fig. 12. The effect of the propellant burning time error on dispersion

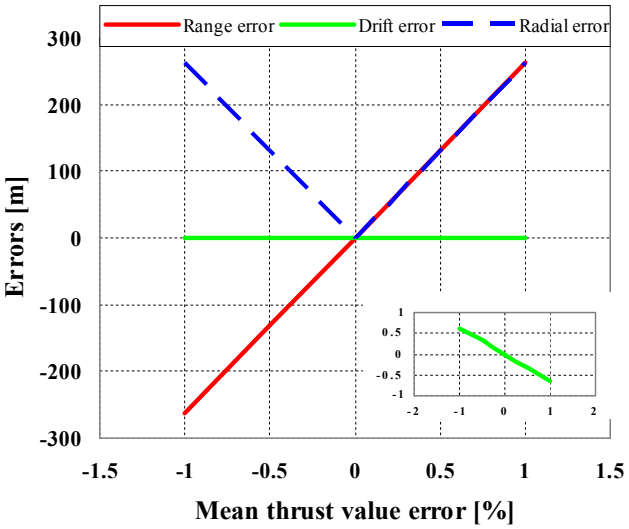

Fig. 13. The effect of the mean thrust error on dispersion

Since it is physically impossible to set the launcher precisely at the desired angle, error in launcher angle is always present where the range error will be decreased or increased depending on the nominal launch angle. In our case study the range decreased and the drift error will be increased as shown in Fig. 14. Increasing the rocket gross mass will decrease the burn-out velocity to decrease the rocket range as shown in Fig. 15.

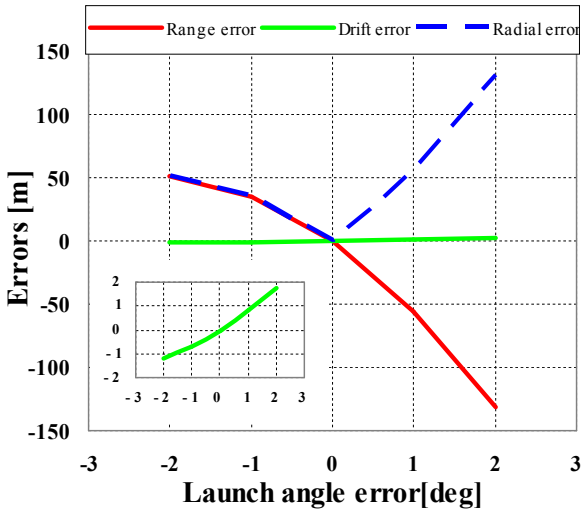

Fig. 14. The effect of rocket launch angle error on dispersion

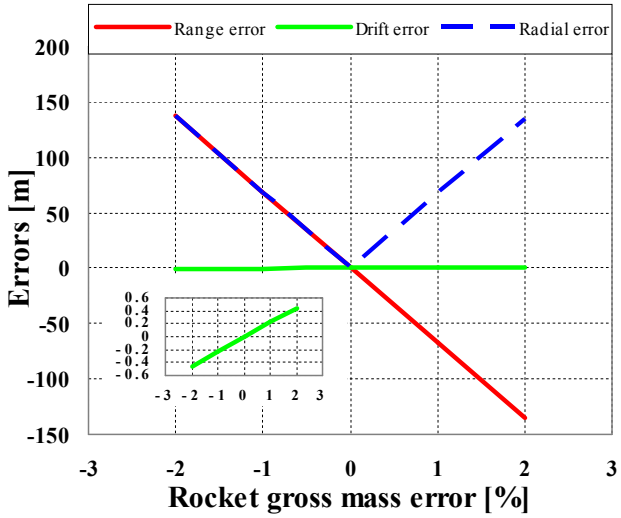

Fig. 15. The effect of the rocket gross mass error on dispersion

Increasing the launch velocity of the rocket will increase the burn-out velocity which will increase the range as shown in Fig. 16. as the launch spinning rate of the rocket is increased the drift will be decreased from its nominal value due to the increasing of rocket stability as shown in Fig. 17. The rocket range increased when a tail wind presented (the rocket Mach no will be decreased) on the rocket body which will decrease the drag force acting on the rocket as shown in Fig. 18. As shown in Fig. 19, if a cross wind is presented the rocket drifts to right if the wind came from right and vise verse due to the presence of tail surfaces behind the rocket center of gravity to make the rocket fly opposite to wind direction.

There is no effect of the axial and lateral mass moments of inertia on the rocket range. But in case of drift, the drift will be decreased with increasing I_{xx} and increased with increasing of I_{yy} (I_{zz}) as shown in Fig.s 20, 21.

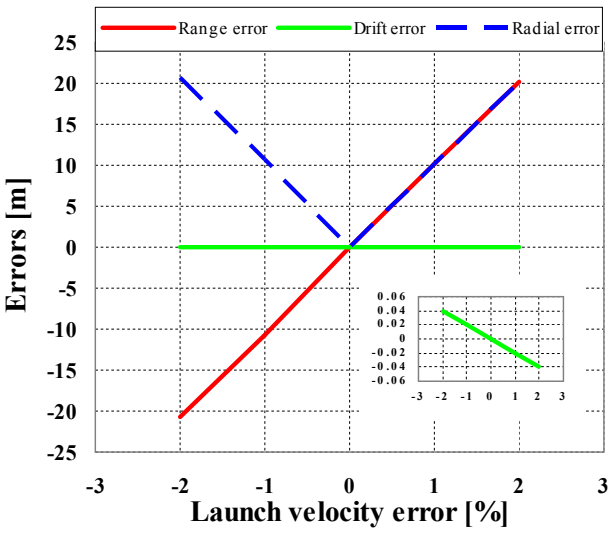

Fig. 16. The effect of launch velocity error on dispersion

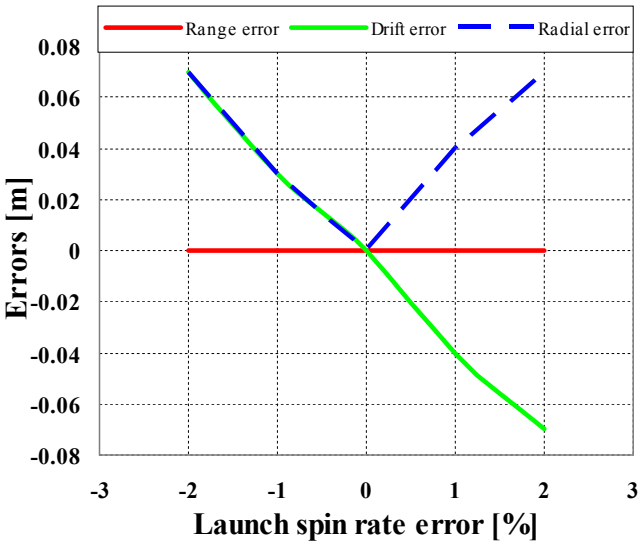

Fig. 17. The effect of launch spin rate error on dispersion

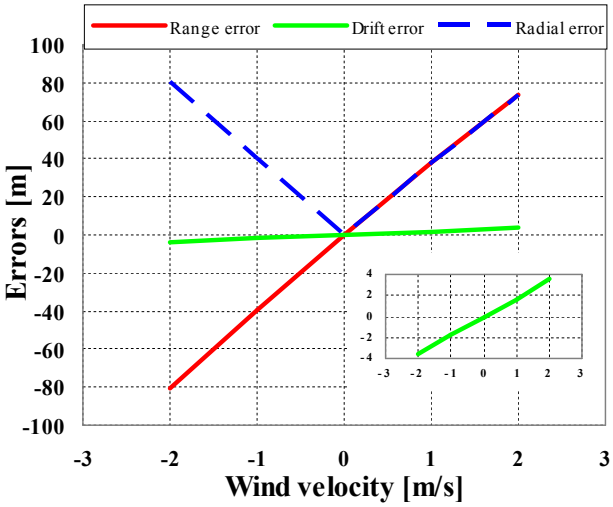

Fig. 18. The effect of wind velocity on dispersion

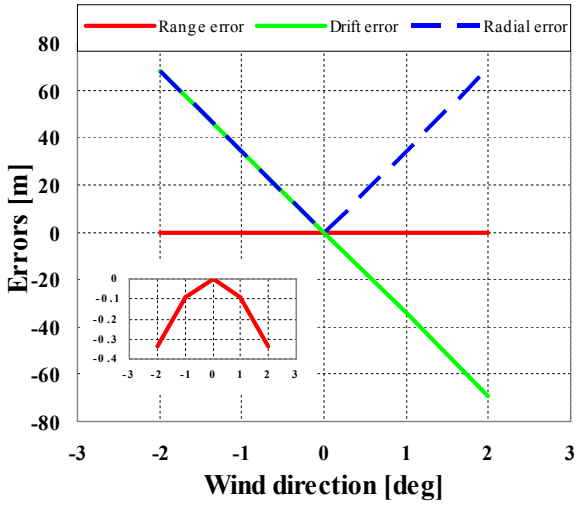

Fig. 19. The effect of wind direction (10 m/s) on dispersion

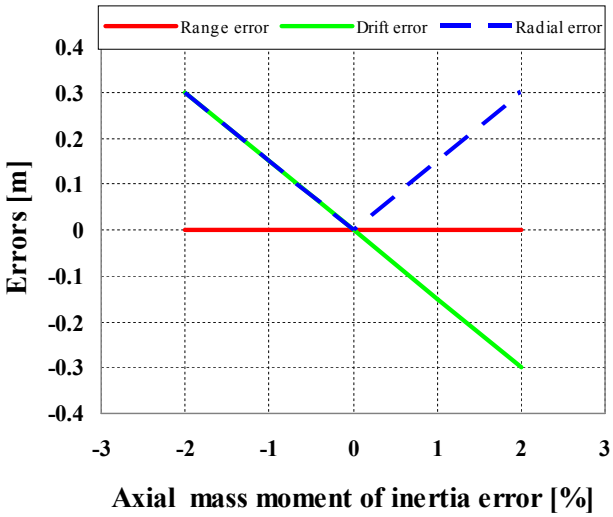

Fig. 20. The effect of axial mass moment of inertia error on dispersion

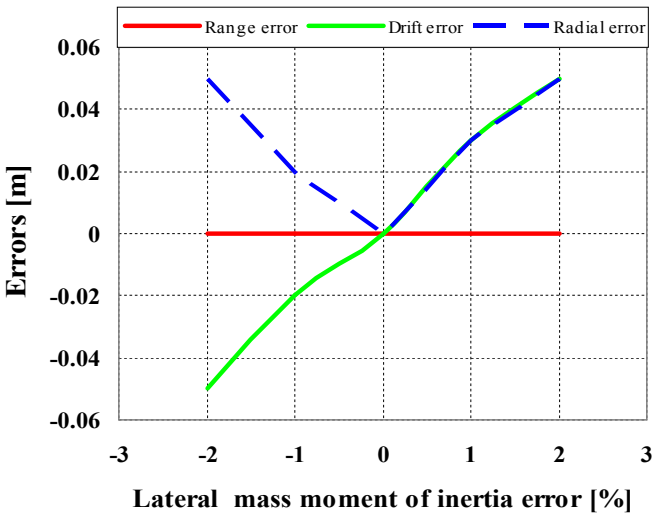

Fig. 21. The effect of lateral mass moment of inertia error on dispersion

4. Conclusion:

Trajectory analysis of an unguided 122mm artillery rocket using simulation software was undertaken to show the importance of this type of analysis in order to know all parameters acting on the rocket during its flight which may be useful to avoid flight mistakes. The dispersion analysis is used to show the importance of identifying the design weaknesses in margins of specific parameters. Also, it is used to find out the optimum values of the rocket motor parameters for lowest impact point error, and the probability of flight-to-target success. Results were presented for the selected conditions in the form of dispersion. This analysis showed that the rocket motor parameters (burning time, propellant mass and mean thrust value) have a great effect on the rocket range and its impact point error.

5. References

[1] Bernard Etkin, “Dynamics of Atmospheric Flight”, United States of America, John Wiley & Sons, 1972.

[2] Douglas O., and Mark C., "Model Predictive Control of a Direct Fire Projectile Equipped With Canards ", *Journal of Dynamic Systems, Measurement, and Control*, *Vol. 130*, NOVEMBER 2008.

[3] Ezeddine Salem Ab. Ali, “Parametric Study Of Missile Trajectory”, M.Sc. thesis, Military Technical College, Cairo, Egypt, March 2009.

[4] Gagnon E., and Lauzon M., "Course Correction Fuze Concept Analysis for In Service 155 mm Spin-Stabilized Gunnery Projectiles", *AIAA Guidance, Navigation and Control Conference and Exhibit*, Honolulu, Hawaii, 18 - 21 August 2008.

[5] Jankovic, S., Gallant, J., and Celens, E., "Dispersion of an Artillery Projectile due to Unbalance", *18th International Symposium on Ballistics*, San Antonio, pp. 128-141, 15-19 November, 1999.

[6] Khalil M. S., “Trajectory Predection of Flying Vehicle“, M.Sc. thesis, Military Technical College, Cairo, Egypt, 2008.

[7] Lua, K. B., Lim, T. T., and Luo, S. C., “Helical-Groove and Circular-Trip Effects on Side Force”, *Journal of Aircraft, Vol.37, No.5*, pp. 906-915, 2000.

[8] SAGHAFI F., and KHALILIDELSHAD M., "A Monte-Carlo Dispersion Analysis of a Rocket Flight Simulation Software", 17th European Simulation Multi-Conference ESM2003, England, 9-11 June, 2003.

[9] Sailaranta, T., Siltavuori, A., Laine, S., and Fagerstrom, B., "On Projectile Stability and Firing Accuracy", *20th International Symposium on Ballistics*, Orlando, pp. 195-202, 23-27 September, 2002.